

# pH Regulates Cation Selectivity of Poly-(*R*)-3-hydroxybutyrate/Polyphosphate Channels from *E. coli* in Planar Lipid Bilayers<sup>†</sup>

S. Das<sup>‡</sup> and R. N. Reusch<sup>\*,§</sup>

Department of Microbiology and Molecular Genetics, Michigan State University, East Lansing, Michigan 48824, and  
Department of Biophysics, University of Delhi South Campus, New Delhi, India

Received September 1, 2000; Revised Manuscript Received December 18, 2000

**ABSTRACT:** Poly-(*R*)-3-hydroxybutyrate/polyphosphate (PHB/polyP) complexes, whether isolated from the plasma membranes of bacteria or prepared from the synthetic polymers, form ion channels in planar lipid bilayers that are highly selective for Ca<sup>2+</sup> over Na<sup>+</sup> at physiological pH. This preference for divalent over monovalent cations is attributed to a high density of negative charge along the polyP backbone and the higher binding energies of divalent cations. Here we modify the charge density of polyP by varying the pH, and observe the effect on cation selectivity. PHB/polyP complexes, isolated from *E. coli*, were incorporated into planar lipid bilayers, and unitary current–voltage relations were determined as a function of pH. When Ca<sup>2+</sup> was the sole permeant cation, conductance diminished steadily from 97 ± 6 pS at pH 7.4 to 47 ± 3 pS at pH 5.5. However, in asymmetric solutions of Ca<sup>2+</sup> and Na<sup>+</sup>, there was a moderate increase in conductance from 98 ± 4 at pH 7.4 to 129 ± 4 pS at pH 6.5, and a substantially larger increase to 178 ± 6 pS at pH 5.6, signifying an increase in Na<sup>+</sup> permeability or disorganization of channel structure. Reversal potentials point to a sharp decrease in preference for Ca<sup>2+</sup> over Na<sup>+</sup> over a relatively small decrease in pH. Ca<sup>2+</sup> was strongly favored over Na<sup>+</sup> at physiological pH, but the channels became nonselective near the pK<sub>2</sub> of phosphate (~6.8), and displayed weak selectivity for Na<sup>+</sup> over Ca<sup>2+</sup> at acidic pH. Evidently, PHB/polyP complexes are versatile ion carriers whose selectivity may be modulated by small adjustments of the local pH. The results may be relevant to the physiological function of PHB/polyP channels in bacteria and the role of PHB and polyP in the *Streptomyces lividans* potassium channel.

The linear homopolymers inorganic polyphosphate (polyP)<sup>1</sup> and poly-(*R*)-3-hydroxybutyrate (PHB) are ubiquitous constituents of biological cells (1–7). PolyP is a polyanion composed of tetrahedral phosphate units joined by flexible phosphoanhydride bonds (8, 9). PHB is an amphiphilic polymer of *R*-3-hydroxybutyrate (10, 11) that forms ion-conducting complexes with salts (12, 13) and nonspecific ion channels in planar lipid bilayers (13). The two polymers associate to form complexes in the plasma membranes of *Escherichia coli* and other bacteria (14–17) that may play a role in Ca<sup>2+</sup> homeostasis (18, 19). PHB/polyP complexes, isolated from bacterial membranes or formed synthetically, create channels in planar lipid bilayers at physiological pH that display the salient characteristics of protein Ca<sup>2+</sup> channels, i.e., voltage dependence, selectivity for divalent over monovalent cations, permeance to Ca<sup>2+</sup>, Sr<sup>2+</sup>, and Ba<sup>2+</sup>, and block by transition metals (20–23). Recently, PHB and polyP were found to be components of

the CaATPase pump of human erythrocytes (24) and the *Streptomyces lividans* K<sup>+</sup> channel (25), suggesting they may be more versatile and more prevalent ion carriers than previously thought.

The simple molecular structures of PHB and polyP make PHB/polyP channels attractive models for investigating molecular mechanisms of ion selection. PolyP attracts and binds all cations; however, it has a known preference for divalent over monovalent cations, attributed to its high density of negative charge at physiological pH, and the higher binding energies of multivalent cations (8, 9). One may assume that lowering the pH would reduce the charge density of polyP, thereby making the complexes less efficient at binding divalent cations and more effective at binding monovalent cations. However, the magnitude of the pH change required to significantly alter the selectivity, and the effect of pH change on channel structure are unknown.

Here we examine the influence of pH on the conductance of PHB/polyP channels and their selectivity for Ca<sup>2+</sup> and Na<sup>+</sup>. These two cations have similar size and coordination geometry (26, 27) and hence may be distinguished primarily by charge. PHB/polyP complexes were isolated from *E. coli* and incorporated into planar lipid bilayers, and the relative permeabilities of Ca<sup>2+</sup> and Na<sup>+</sup> were determined as a function of pH. The results indicate that surprisingly small variations in pH close to physiological values transform PHB/polyP complexes from channels that are highly selective for Ca<sup>2+</sup> to channels that are weakly selective for Na<sup>+</sup>.

<sup>†</sup> Supported by NSF Grant MCB-9816053.

<sup>\*</sup> Address correspondence to this author at the Department of Microbiology and Molecular Genetics, Giltner Hall, Michigan State University, East Lansing, MI 48824. Tel.: (517) 355-9307. FAX: (517) 353-8957. Email: rnreusch@msu.edu.

<sup>‡</sup> University of Delhi South Campus.

<sup>§</sup> Michigan State University.

<sup>1</sup> Abbreviations: PHB, poly-(*R*)-3-hydroxybutyrate; polyP, inorganic polyphosphate; Hepes, 4-(2-hydroxyethyl)-1-piperazineethanesulfonic acid; Mes, 4-morpholineethanesulfonic acid; Tris, 2-amino-2-(hydroxymethyl)-1,3-propanediol; POPC, 1-palmitoyl-2-oleoylphosphatidylcholine.

## EXPERIMENTAL PROCEDURES

**Media.** SOB medium (28): 2% Bacto-tryptone (Difco), 0.5% yeast extract (Difco), 10 mM NaCl, 2.5 mM KCl. Transformation buffer: 100 mM KCl, 45 mM MnCl<sub>2</sub>, 10 mM CaCl<sub>2</sub> in 10 mM Mes neutralized to pH 6.3 with KOH.

**Preparation of Competent Cells of *E. coli* DH5 $\alpha$ .** *E. coli* DH5 $\alpha$  cells were made genetically competent by a variation of the method of Hanahan (28) as previously described (16). This procedure has been shown to effect a 50–100-fold increase in the concentration of complexes in the plasma membranes (16, 17). Briefly, cells were cultured in SOB medium to an absorbance at 550 nm of ca. 0.4. The cells were pelleted at low centrifugal speed (800g) for 10 min at 4 °C, and gently resuspended in 1/3 volume of transformation buffer for 30 min at 4 °C. The cells were then collected under the same conditions as above.

**Extraction of PHB/PolyP Complexes from *E. coli*.** The pellet of *E. coli* competent cells was washed with methanol (2 $\times$ ), methanol/acetone 1:1 (2 $\times$ ), and acetone (2 $\times$ ), and the dry residue was extracted overnight at 4 °C with chloroform (10<sup>9</sup> cells/mL of CHCl<sub>3</sub>). Since the complexes are sensitive to temperature and moisture, all solvents were ice-cold and dried with Molecular Sieves—3 Å for alcohol and acetone, and 4 Å for chloroform (Aldrich).

**Incorporation of PHB/PolyP Channels into Lipid Bilayer Membranes.** Lipid bilayer membranes were formed across an aperture of  $\sim$ 150  $\mu$ m diameter in a Delrin cup (Warner Instruments) with a lipid mixture of synthetic 1-palmitoyl-2-oleoylphosphatidylcholine (POPC)(Avanti Polar Lipids) and cholesterol (7:1 w/w) in decane. The bilayers were formed between aqueous bathing solutions, the composition of which is described under Results. All salts used in the bathing solutions were ultrapure (>99%) (Aldrich). PHB/Ca-polyP complexes were incorporated into the bilayer by direct addition to the lipids before forming the bilayer; 1–2  $\mu$ L of a chloroform solution of the complexes was added to 250  $\mu$ L of decane solution of the above lipids (ratio of PHB to phospholipid was <1:1000), and after removal of chloroform by evaporation with a stream of dry nitrogen gas, the solution was used to form a bilayer.

**Recording and Data Analyses.** Unitary currents were recorded with an integrating patch clamp amplifier (Axopatch 200A, Axon Instruments). The cis solution (voltage command side) was connected to the head-stage input, and the trans solution was held at virtual ground via a pair of matched Ag–AgCl electrodes. Currents through the voltage-clamped bilayers (background conductance <6 pS) were low-pass-filtered at 10 kHz (–3 dB cutoff, Bessel type response) and recorded on videocassettes after digitization through an analog-to-digital converter (VR 10B, Instrutech Corp.). Using standard voltage conventions, positive clamping potentials are quoted as potentials with respect to the ground (trans chamber), and positive currents are shown as “upward” deflections in the traces.

Data were analyzed offline after filtration through an 8 pole Bessel filter (902LPF, Frequency Devices) at 1–2 kHz as mentioned in the figure legends using pClamp software (version 6.0.4, Axon Instruments), with additional standard nonlinear fitting routines where necessary. Sampling was done using a TL-1 interface (Axon Instruments) at 5–20 kHz. Channel amplitudes and the proportion of time spent

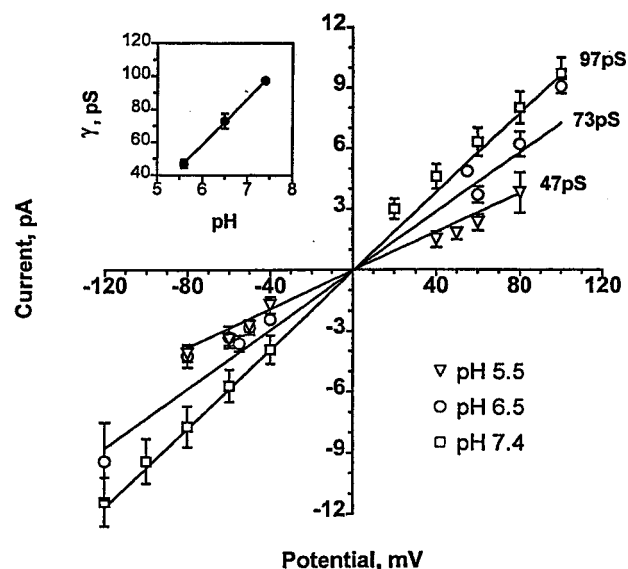


FIGURE 1: Unitary current–voltage relationships of *E. coli* PHB/polyP channels in planar bilayers between symmetric Ca<sup>2+</sup> solutions at various pHs. PHB/polyP complexes were isolated from *E. coli* and incorporated into planar bilayers of synthetic POPC and cholesterol (7:1 w/w) between symmetric bathing solutions of 200 mM CaCl<sub>2</sub>, 5 mM MgCl<sub>2</sub>, 10 mM buffer at 22 °C. Tris–Hepes was used as buffer at pH 7.4, Mes at pH 6.5, and NaOAc at pH 5.5. All points amplitude histograms were constructed for single channel records at each indicated potential. Data were filtered at 1 kHz. The points show the mean peak position of Gaussian distributions, fit by a simplex least-squares procedure at respective clamping potentials. The data shown here are mean amplitudes of the major open state obtained from 3–5 independent experiments. Indicated single channel conductances represent the slope of the best fit obtained by linear regression. The bars represent the standard deviation of data. Indicated unitary conductances represent the slope of the best fit obtained by linear regression. The inset shows the pH dependence of unitary conductance ( $\gamma$ ) of the PHB/polyP channel.

in individual conductance states were measured by fitting multiple Gaussian distributions to all point amplitude histograms. The data for asymmetric solutions have been corrected for the junction potential (–12 mV).

## RESULTS

**Gating of PHB/PolyP Channels.** In planar bilayer membranes, PHB/polyP channels display two principal modes of gating, which are postulated to originate from two preferred conformations of the complexes (22). Under the conditions used in our studies, the channel is observed >90% of the time in mode 2; consequently, we report values for the most frequently observed independent unitary conductance in mode 2.

**pH-Dependence of Ca<sup>2+</sup> Conductance in Symmetric Solutions.** We first examined the current–voltage relations of PHB/polyP channels as a function of pH in symmetric solutions containing Ca<sup>2+</sup> as the primary conducting cation. PHB/polyP complexes were isolated from *E. coli* competent cells and incorporated into planar bilayers of POPC/cholesterol (7:1 w/w) between bathing solutions of 200 mM CaCl<sub>2</sub>, 5 mM MgCl<sub>2</sub>, and 10 mM buffer. Tris–Hepes was used as buffer at pH 7.4, Mes at pH 6.5, and NaOAc at pH 5.5.

Figure 1 summarizes the data from several independent measurements. The inset shows the linear dependence of

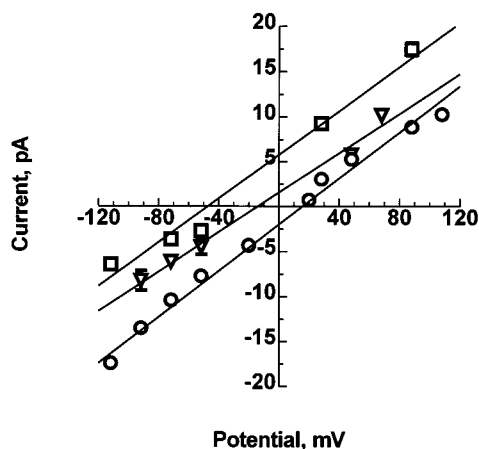


FIGURE 2: Current–voltage relationships of *E. coli* PHB/polyP channels in planar bilayers between asymmetric solutions of  $\text{Ca}^{2+}$  and  $\text{Na}^{+}$  at representative pHs. PHB/polyP complexes were isolated from *E. coli* and incorporated into planar bilayers of synthetic POPC and cholesterol (7:1 w/w) between asymmetric bathing solutions of 65 mM  $\text{CaCl}_2$ , 10 mM  $\text{NaCl}$ , 5 mM  $\text{MgCl}_2$ , 10 mM buffer (cis side) and 200 mM  $\text{NaCl}$ , 1 mM  $\text{CaCl}_2$ , 5 mM  $\text{MgCl}_2$ , 10 mM buffer (trans side) at 22 °C. Tris–Hepes was used as buffer at pH 7.6, 7.4, and 7.0; Mes at pH 6.5; and NaOAc at pH 5.6. The data shown have been corrected for the junction potential (–12 mV). All points amplitude histograms were constructed for single channel records at each indicated potential. Data were filtered at 1 kHz. The points show the mean peak position of Gaussian distributions, fit by a simplex least-squares procedure at respective clamping potentials. The data shown here are mean amplitudes of the major open state obtained from 3–5 independent measurements at each of three pH values. Indicated single channel conductances represent the slope of the best fit obtained by linear regression. The error bars represent the standard deviation of the data around the mean amplitude of the fitted Gaussian distributions. Error bars are not visible when they are smaller than the symbol size. Symbols are pH 5.5 ( $\nabla$ ), pH 6.5 ( $\circ$ ), and pH 7.4 ( $\square$ ).

channel conductance on pH. The single-channel  $\text{Ca}^{2+}$  conductance decreased consistently from  $97 \pm 3$  pS at pH 7.4 to  $73 \pm 3$  pS at pH 6.5 to  $47 \pm 3$  pS at pH 5.5. This suggests that the channels become less efficient in binding and transporting  $\text{Ca}^{2+}$  as the charge density on polyP is attenuated.

**pH-Dependence of Unitary Conductance in Asymmetric Solutions.** Next we determined the total ( $\text{Ca}^{2+} + \text{Na}^{+}$ ) unitary conductance of PHB/polyP as a function of pH. PHB/polyP complexes were incorporated into planar bilayer membranes, composed of POPC and cholesterol (7:1 w/w), between asymmetric bathing solutions of 65 mM  $\text{CaCl}_2$ , 10 mM  $\text{NaCl}$ , 5 mM  $\text{MgCl}_2$ , 10 mM buffer (cis side) and 200 mM  $\text{NaCl}$ , 1 mM  $\text{CaCl}_2$ , 5 mM  $\text{MgCl}_2$ , 10 mM buffer (trans side) at 22 °C. Tris–Hepes was used as buffer at pH 7.6, 7.4, and 7.0, Mes at pH 6.5, and NaOAc at pH 5.6.

Representative current–voltage relationships are shown for three pH values in Figure 2. The most frequently observed unitary gating unit at pH 7.4 had a conductance of  $98 \pm 4$  pS, although rare events were also observed with a smaller conductance of  $25 \pm 2$  pS. The slope conductances at various pH, determined graphically from current–voltage relations, are shown in Figure 3. In contrast to the decrease in conductance observed with declining pH in symmetric solutions, the conductance of PHB/polyP channels in asymmetric solutions remained generally in the same range from pH 7.6 to 6.5 (98–129 pS), with a minimum at pH 7.4. There was, however, a substantial increase in conductance to 178

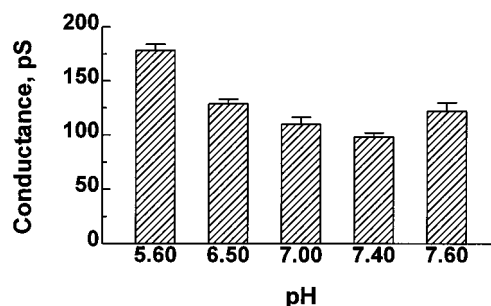


FIGURE 3: Unitary conductance of *E. coli* PHB/polyP channels between asymmetric solutions of  $\text{Ca}^{2+}$  and  $\text{Na}^{+}$  as a function of pH. Experimental conditions were the same as in Figure 2 above. Values for unitary channel conductances represent the slope of the best fit obtained by linear regression at each pH in asymmetric solution obtained from 3–5 independent measurements. The bars represent the standard deviation of the data.

$\pm 6$  pS when the pH was decreased to 5.6. This increase in conductance at acidic pH, despite a diminishing  $\text{Ca}^{2+}$  conductance as shown above for symmetric solutions, could arise from an increase in  $\text{Na}^{+}$  conductance or disorganization of the channel structure.

**pH-Dependence of Cation Selectivity.** Previous studies have shown that PHB/polyP channels demonstrate a strong selectivity for  $\text{Ca}^{2+}$  over  $\text{Na}^{+}$  at pH 7.4 (20, 21). This selectivity was now examined as a function of pH. Reversal potentials (Figure 5) and zero currents (Figure 6) were determined from current–voltage relationships in lipid bilayers between asymmetric solutions of  $\text{Ca}^{2+}$  and  $\text{Na}^{+}$  at various pHs as described above. Representative traces near the reversal potential are shown in Figure 4. The Nernst equilibrium potentials calculated from concentrations for this system are  $E_{\text{Ca}} = -53$  mV,  $E_{\text{Cl}} = +7$  mV, and  $E_{\text{Na}} = +76$  mV.

As can be seen in Figure 5, the reversal potential is very sensitive to pH. At physiological pH, the reversal potential was  $-42$  mV, close to  $E_{\text{Ca}}$ , indicating a strong preference for  $\text{Ca}^{2+}$  over  $\text{Na}^{+}$ , in agreement with earlier reports (20, 21). However, at neutral pH, the reversal potential is close to zero, indicating that the channels are essentially nonselective. Apparently, the complexes undergo a sharp decrease in preference for  $\text{Ca}^{2+}$  within a relatively small pH window near physiological values. Reversal potentials turn moderately positive as the pH decreases further, leveling off at pH 6.5. This indicates that the channels become weakly selective for  $\text{Na}^{+}$  over  $\text{Ca}^{2+}$  at acidic pH, but the preference for monovalent cations does not significantly improve when the pH is reduced below 6.5. The zero currents show a strong but opposite dependence on pH, decreasing linearly with decreasing pH, but also leveling off at pH 6.5 (Figure 6).

## DISCUSSION

The present studies show that the conductance of PHB/polyP channels and their selectivity for  $\text{Ca}^{2+}$  over  $\text{Na}^{+}$  are very sensitive to small variations in pH. PHB/polyP complexes in planar bilayers are transformed from strongly  $\text{Ca}^{2+}$ -selective channels at physiological pH to nonselective channels at pH  $\sim 7.0$ , and become weakly  $\text{Na}^{+}$ -selective channels at pH  $< 7.0$ . This remarkable shift in preference from divalent to monovalent cations over a narrow pH range near physiological values provides the basis for a molecular



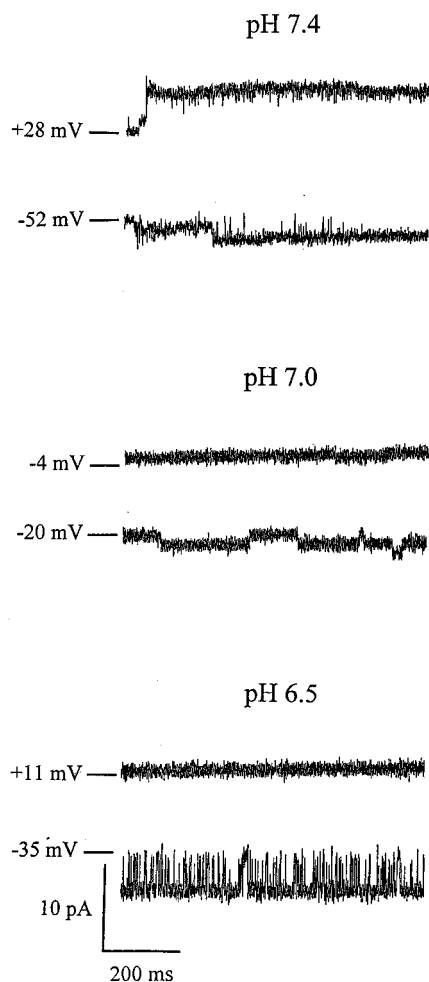


FIGURE 4: Representative current traces near the reversal potential of *E. coli* PHB/polyP channels at various pHs. Experimental conditions were the same as in Figure 2 above. The current traces were filtered through an eight pole Bessel filter at 1 kHz and sampled at 10 kHz. The clamping potentials are indicated at the left. The bars at the left indicate the position of the baseline.

mechanism by which cation transport across biological membranes may be regulated.

The  $\text{Ca}^{2+}$  and  $(\text{Ca}^{2+}+\text{Na}^+)$  conductances were each determined as a function of pH. It has been demonstrated previously that PHB/polyP channels, isolated from *E. coli* plasma membranes and incorporated into planar lipid bilayers, are permeant to  $\text{Ca}^{2+}$  at physiological pH (20, 21). This is confirmed by the data in Figure 1, which show a  $\text{Ca}^{2+}$  conductance, determined from current–voltage relationships in symmetric solutions at pH 7.4, of  $97 \pm 7$  pS. When the pH was reduced in steps from 7.4 to 5.5, the  $\text{Ca}^{2+}$  conductance decreased steadily to  $47 \pm 3$  pS, signifying a progressive reduction in the permeability of the channels to  $\text{Ca}^{2+}$ . On the other hand,  $(\text{Ca}^{2+}+\text{Na}^+)$  conductance, determined from current–voltage relationships in asymmetric solutions (Figure 2), exhibited a moderate increase from  $98 \pm 4$  pS at pH 7.4 to  $129 \pm 4$  pS at pH 6.5 and a more substantial increase to  $178 \pm 6$  pS at pH 5.6 (Figure 3). Apparently, lowering the charge density on polyP diminishes the ability of PHB/polyP to transport divalent cations, but at the same time makes them somewhat more efficient carriers of monovalent cations. This increase in conductance at acidic pH may reflect the lower hydration enthalpy of  $\text{Na}^+$  as compared to  $\text{Ca}^{2+}$  (103.5 vs 394 kcal/mol) (27, 28) and

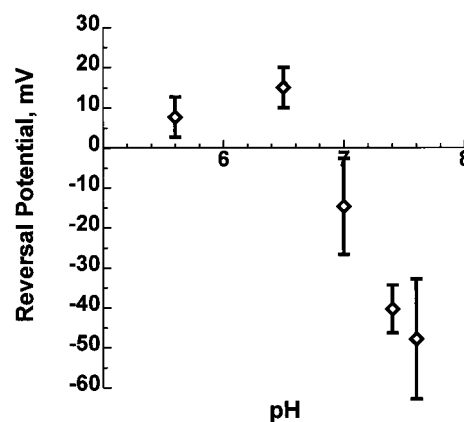


FIGURE 5: pH-dependence of reversal potentials of *E. coli* PHB/polyP channels between asymmetric solutions of  $\text{Ca}^{2+}$  and  $\text{Na}^+$ . Experimental conditions were the same as in Figure 2. Reversal potentials were determined from the intersection of the fitted current–voltage curves with the potential axis. Each point represents the data from 3–5 experiments. The error bars show the 95% confidence level of the data. For details of analysis, see the legend of Figure 2 and Experimental Procedures.

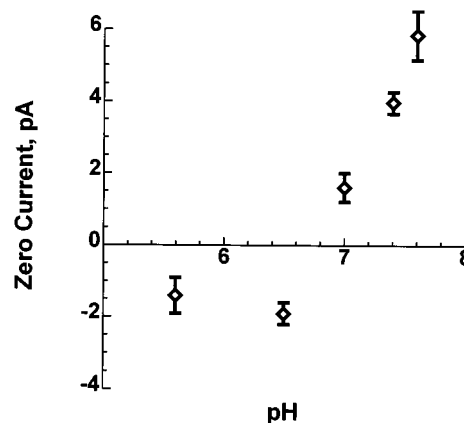


FIGURE 6: pH-dependence of zero currents for PHB/polyP channels between asymmetric solutions of  $\text{Ca}^{2+}$  and  $\text{Na}^+$ . Experimental conditions were the same as in Figure 2 above. Zero currents were determined from the intersection of the fitted current–voltage curve with the current axis at 0 mV clamping potential. For details of the analysis, see the legend of Figure 2 and Experimental Procedures. Each point represents the data from 3–5 experiments. The error bars show the standard deviation of the data.

perhaps a less ordered and more open conformation for the channel.

The results demonstrate clearly that the selectivity of PHB/polyP channels for  $\text{Ca}^{2+}$  vs  $\text{Na}^+$  is decisively modulated by pH (Figures 3–6). At physiological pH, PHB/polyP channels display a strong preference for  $\text{Ca}^{2+}$  over  $\text{Na}^+$ , as evidenced by reversal potentials in the range of  $\sim -42$  pS (Figure 5), close to the Nernst equilibrium potential of  $-53$  mV. This preference for  $\text{Ca}^{2+}$  subsides within half a pH unit. Evidently, lowering the pH not only decreases  $\text{Ca}^{2+}$  conductance but also abolishes the preference for  $\text{Ca}^{2+}$  over  $\text{Na}^+$ . At acidic pH, the channels display a weak preference for  $\text{Na}^+$  over  $\text{Ca}^{2+}$ . The reversal potentials suggest that the preference for  $\text{Na}^+$  levels off near pH 6.5 (Figure 6). Further improvement in selectivity may be prevented by structural disorganization at low pH. The zero currents (Figure 6) indicate that, given similar ion gradients, membrane depolarization would result in an inward flow of  $\text{Ca}^{2+}$  at pH 7.4, no net ion flow at pH 7.0, and an outward flow, containing somewhat more  $\text{Na}^+$

than  $\text{Ca}^{2+}$ , at pH 6.5.

The selectivity of PHB/polyP complexes for  $\text{Ca}^{2+}$  and  $\text{Na}^{+}$  is largely attributable to (1) the physical properties of polyP, in particular its high charge density and conformational polymorphism, and (2) cation binding energies. Phosphates are trivalent with  $\text{pKs}$  approximately 5 units apart at  $\sim 2$ , 6.8, and 12 (8); consequently, even after they are linked together, each subunit bears a negative charge at physiological pH. In aqueous solution, polyPs have a titratable strong-acid hydrogen atom for each subunit and a titratable weak-acid hydrogen atom corresponding only to the terminal subunits. In the channel, most of the polyP is enclosed within a PHB sheath, but its terminal units remain in an aqueous environment. The cation binding sites on polyP, unlike those of many chelating agents, do not have rigid ligand geometries. The low energy barrier to rotation about the P—O—P bond connecting the subunits allows the tetrahedra to twist into a variety of different conformations to correspond to the binding preferences of approaching cations (8, 9). Since there is no advantage to size or coordination geometry, cations with multiple charges are selected, due to their higher binding energies. Part of the hydration shell of the cations is removed on binding to polyP, and the remaining water molecules may then be replaced by the ester carbonyl oxygens of PHB, in stepwise fashion, as they enter binding cavities formed by the phosphoryl oxygens of polyP and the ester carbonyl oxygens of PHB. When bound cations move into the channel, size and coordination geometry may become determining factors. These properties were not significant in this study since  $\text{Ca}^{2+}$  and  $\text{Na}^{+}$  are comparable in size (1.06 Å vs 0.98 Å) and coordination preferences (26, 27).

From the above, we can conclude that the striking change in permeability of the complexes with reduction in pH observed in this study can be attributed largely to the effects of pH on the ionization of polyP subunits. When the charge density of polyP is high, i.e., above  $\text{pK}_2$  ( $\sim 6.8$ ), as at physiological pH, polyP will preferentially bind  $\text{Ca}^{2+}$  over  $\text{Na}^{+}$ . At pH below  $\text{pK}_2$ , a lower charge density reduces the ability of polyP to bind multivalent cations, effecting an increased binding of monovalent cations such as  $\text{Na}^{+}$ .

The transformation of PHB/polyP channels from  $\text{Ca}^{2+}$ -selective to  $\text{Na}^{+}$ -permeant carriers over a narrow pH range, near cellular pH, may have widespread physiological implications. Local pH near polyP termini can be altered in vivo by a proton flow in close proximity to or through PHB/polyP complexes, or by strategic placement of basic amino acid residues of associated proteins. The latter was suggested as a mechanism for selection of  $\text{K}^{+}$  in the *Streptomyces lividans* potassium channel KcsA (25). It was proposed that arginines at the C-intracellular ends of the channel modulate the negative charge density of terminal polyP units, thus inhibiting the binding of divalent cations and increasing the

permeability of monovalent cations. Refinement of the selectivity for  $\text{K}^{+}$  over  $\text{Na}^{+}$  could then be accomplished by fine-tuning the size of cation binding cavities within the channel by adjusting the distance between PHB and polyP. Evidently, PHB/polyP complexes have unique characteristics that enable them to act in concert with proteins to achieve selective transmembrane transport of specific cations.

## REFERENCES

1. Reusch, R. N. (1992) *FEMS Microbiol. Rev.* 103, 119–130.
2. Müller, H. M., and Seebach, D. (1994) *Angew. Chem.* 32, 477–502.
3. Reusch, R. N., and Gruhn, A. G. (1997) *Int. Symp. Bact. Polyhydroxyalkanoates*, 1996, 10–19.
4. Seebach, D., Brunner, A., Bachmann, B., Hoffmann, T., Kühnle, F. N., and Lengweiler, U. D. (1996) *Ernst Schering Res. Found. Workshop* 28, 1–105.
5. Kulaev, I. S. (1979) *The Biochemistry of Inorganic Polyphosphates* (Brookes, R. F., Ed.) John Wiley and Sons, New York.
6. Wood, H. G., and Clark, J. E. (1988) *Annu. Rev. Biochem.* 57, 235–260.
7. Kornberg, A. (1999) *Prog. Mol. Subcell. Biol.* 23, 1–18.
8. Corbridge, D. E. C. (1985) *Stud. Inorg. Chem.* 6, 170–178.
9. Majling, J., and Hanic, F. (1980) *Top. Phosphorus Chem.* 10, 41–502.
10. Anderson, A. J., and Dawes, E. A. (1990) *Microbiol. Rev.* 54, 450–472.
11. Doi, Y. (1990) *Microbial Polyesters*, VCH, New York.
12. Bürger, H. M., and Seebach, D. (1993) *Helv. Chim. Acta* 76, 2570–2580.
13. Reusch, R. N., and Reusch, W. H. (1993) U.S. Patent No. 5,266,422.
14. Seebach, D., Brunner, A., Bürger, H. M., Reusch, R. N., and Bramble, L. L. (1996) *Helv. Chim. Acta* 79, 507–517.
15. Reusch, R. N., and Sadoff, H. L. (1983) *J. Bacteriol.* 156, 778–788.
16. Reusch, R. N., Hiske, T. W., and Sadoff, H. L. (1986) *J. Bacteriol.* 168, 553–562.
17. Reusch, R. N., and Sadoff, H. L. (1988) *Proc. Natl. Acad. Sci. U.S.A.* 85, 4176–4180.
18. Holland, I. B., Jones, H. E., Campbell, A. K., and Jacq, A. (1999) *Biochimie* 81, 901–907.
19. Jones, H. E., Holland, I. B., Baker, H. L., and Campbell, A. K. (1999) *Cell Calcium* 25, 265–274.
20. Reusch, R. N., Huang, R., and Bramble, L. L. (1995) *Biophys. J.* 69, 754–766.
21. Das, S., Lengweiler, U. D., Seebach, D., and Reusch, R. N. (1997) *Proc. Natl. Acad. Sci. U.S.A.* 94, 9075–9079.
22. Das, S., and Reusch, R. N. (1999) *J. Membr. Biol.* 170, 135–145.
23. Das, S., Kurcok, P., Jedlinski, Z., and Reusch, R. N. (1999) *Macromolecules* 32, 8781–8785.
24. Reusch, R. N., Huang, R., and Kosk-Kosicka, D. (1997) *FEBS Lett.* 412, 592–596.
25. Reusch, R. N. (1999) *Biochemistry* 38, 15666–15672.
26. Lehn, J. (1973) *Struct. Bonding (Berlin)* 10, 1–24.
27. Simon, W., Morf, W. E., and Meier, P. C. (1973) *Struct. Bonding (Berlin)* 16, 113–160.
28. Hanahan, D. (1983) *J. Mol. Biol.* 166, 557–580.

BI0020776